2025 25th International Conference on Process Control (PC)
June 3–6, 2025, Štrbské Pleso, Slovakia

Rate-limited spacecraft attitude maneuvers with Linear Reference Governor approach

1st Dominik Beňo
Space division
VZLU AEROSPACE
Prague, Czechia
0000-0001-5359-8585

2nd Dávid Hriadel
Space division
VZLU AEROSPACE
Prague, Czechia
0009-0005-7646-2927

3rd Juraj Wolf
Space division
VZLU AEROSPACE
Prague, Czechia
0009-0002-7852-9038

***Abstract*—This paper presents a Linear Reference Governor (LRG) approach to rate-limited spacecraft attitude maneuvers, addressing the constraints imposed by reaction wheel torque and spacecraft angular velocity. By formulating the problem as an Optimal Control Problem (OCP), the LRG modifies quaternion and angular rate references for a closed-loop system with a state-feedback attitude controller. The method leverages linear approximations, leading to a Quadratic Programming (QP) problem that could be solved onboard VZLU AEROSPACE's upcoming mission. Simulation results demonstrate significant improvements in maneuver duration compared to standard quaternion-based trajectory generation while maintaining adherence to reaction wheel torque constraints. The proposed solution advances spacecraft agility and operational efficiency in challenging mission scenarios.**

***Index Terms*—attitude control, linear control systems, reference governor, constrained control, quaternion kinematics, cubesat**

I. Introduction

Spacecraft maneuvering occurs regularly during the mission lifetime when the spacecraft must switch between its objectives. As an example typical for smaller satellites, the entire spacecraft is re-oriented to align its antenna with the ground segment for high-speed downlink transmission following payload data acquisition at a different attitude. The maneuver must be often performed swiftly, but it should also respect the spacecraft's operational constraints. In that case, it is desired to command the feasible torque of the actuators, but limit the angular rate (e.g. to prevent star tracker loss of acquisition).

There are multiple solutions to constrained spacecraft reorientation. The feasible trajectory towards the desired attitude can be found by path-planning in discretized quaternion space [1], [2]. Exclusion zone avoidance and angular rate limits can be incorporated into the trajectory, but the spacecraft dynamics is neglected.

Next, the attitude controller can be augmented so that angular velocity is constrained [3]. Reference [4] proposed an attitude controller respecting pointing direction constraints using attractive and repulsive artificial potentials. The control law is designed to respect the actuator torque constraints.

This project result was developed within the institutional support of the Ministry of Industry and Trade of the Czech Republic directed to the development of research organizations.

Constrained attitude trajectory can be found by solving optimization problem in the Model Predictive Control (MPC) framework. In particular, the Reference Governor (RG) approach demonstrated the ability to solve the attitude maneuver considering exclusion zone, angular rate, and torque constraints [5], [6]. In both works, the RG solves the nonlinear MPC problem with a pre-stabilized attitude control loop by finding the optimal attitude controller reference.

VZLU AEROSPACE develops Attitude and Orbit Control System (AOCS) for upcoming Cubesat mission with stringent agility and pointing requirements. The spacecraft is built on a versatile platform supporting numerous mission objectives such as celestial and terrestrial camera observation and high-speed terrestrial communication. This work is motivated by increasing the mission availability by reducing the time needed to perform the slew maneuver between desired attitudes while respecting spacecraft operational constraints.

A. Contribution

This paper proposes a Linear Reference Governor (LRG) to solve the attitude maneuvering problem with reaction wheel torque and angular rate constraints. We provide a step-by-step guide on the formulation of the Optimal Control Problem (OCP), considering a pre-stabilized attitude control loop with a Linear-Quadratic Regulator (LQR) controller with quaternion and angular rate reference inputs. The intention is to use the slower inner loop, with an LQR controller, for precise pointing. During maneuvers, the LRG will be enabled and will alter the reference for a slower inner loop. The implemented control scheme is depicted in the Fig. 1.

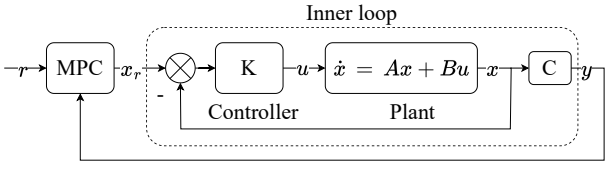

Fig. 1. Control problem scheme

The number of LRG manipulated variables is reduced only to quaternion reference by exploiting the relationship between

the quaternion increments and angular rate. Since the problem is approximated with linear models, the OCP is formulated as Quadratic Programming (QP) which can be efficiently solved, possibly in real-time on the embedded devices. The LRG performance is then compared to the quaternion path-generation method, widely used in space based on Spherical Linear Interpolation (SLERP). The performance of the solution is demonstrated in the high-fidelity simulation.

B. Paper outline

The paper is structured in the following manner. In section II, relevant control-oriented models are introduced, together with default trajectory generation and attitude control functions of the AOCS. Section III describes the design of the reference governor and the derivation of the matrices needed to formulate the OCP. In section IV, the performance results of the reference governor in the numerical simulation are shown and discussed.

II. Problem statement

The spacecraft for which the LRG algorithm is designed is a 6U Cubesat with two attached solar array appendages connected through one-degree-of-freedom joints. Spacecraft rotation and rotation rate estimates are provided by the star tracker measurements or by fusion of the Sun sensor, magnetometer, and gyroscope measurements if the star tracker is blinded. Actuation is performed via a set of four reaction wheels in a pyramidal configuration.

A. Spacecraft model

Spacecraft rigid-body dynamics is given by the Euler rotational equation

$$\boldsymbol{J}_B\,\dot{\boldsymbol{\omega}}_I = \boldsymbol{L}_{\text{ext}} - \boldsymbol{\omega}_I \times \boldsymbol{h}, \tag{1}$$

where $\boldsymbol{J}_B$ is the tensor of inertia, and $\boldsymbol{\omega}_I$ represents the angular velocity vector of the satellite body with respect to the Earth-centered inertial (ECI) frame, expressed in the body frame. The $\boldsymbol{h}$ stands for the angular momentum of the spacecraft [7]. Disturbances and control torques acting on the spacecraft, are represented by symbol $\boldsymbol{L}_{\text{ext}}$. The dynamics of the solar array appendages is neglected in the design model (1).

Spacecraft attitude is described by quaternion attitude kinematics (2).

$$\begin{aligned}\dot{\boldsymbol{q}} &= \frac{1}{2}\begin{pmatrix} q_0 & -q_1 & -q_2 & -q_3 \\ q_1 & q_0 & -q_3 & q_2 \\ q_2 & q_3 & q_0 & -q_1 \\ q_3 & -q_2 & q_1 & q_0 \end{pmatrix}\begin{pmatrix} 0 \\ \boldsymbol{\omega} \end{pmatrix} \\ &\equiv \frac{1}{2}\boldsymbol{Q}(\boldsymbol{q})\begin{pmatrix} 0 \\ \boldsymbol{\omega} \end{pmatrix}\end{aligned} \tag{2}$$

State vector consists of seven state variables, $\boldsymbol{x} = (\omega_x, \omega_y, \omega_z, q_0, q_1, q_2, q_3)^T$. The first trio of state variables, marked as $\boldsymbol{x}_\omega$ corresponds to the angular velocity $\boldsymbol{\omega}_I$. Another four state variables marked $\boldsymbol{x}_q$ correspond to the quaternion $\boldsymbol{q}$ [8]. The state-space representation of the system is given by

$$\begin{aligned}\dot{\boldsymbol{x}}_\omega &= \boldsymbol{J}_B^{-1}(\,\boldsymbol{L}_{\text{ext}} - \boldsymbol{x}_\omega \times \boldsymbol{h}), \\ \dot{\boldsymbol{x}}_q &= \frac{1}{2}\boldsymbol{Q}(\boldsymbol{x}_q)\,(0 \quad \boldsymbol{x}_\omega)^T.\end{aligned} \tag{3}$$

After linearizing the system (3) at $\boldsymbol{x}_0 = (0,0,0,1,0,0,0)^T$ a linear state space model, used in this paper, is obtained as

$$\begin{aligned}\dot{\boldsymbol{x}} &= \boldsymbol{A}\,\boldsymbol{x} + \boldsymbol{B}\,\boldsymbol{u}, \\ \boldsymbol{y} &= \boldsymbol{C}\,\boldsymbol{x}, \\ \boldsymbol{A} &= \begin{pmatrix} \boldsymbol{0}_{4\times3} & \boldsymbol{0}_{4\times3} \\ \frac{1}{2}\boldsymbol{I}_3 & \boldsymbol{0}_{3\times4} \end{pmatrix}, \\ \boldsymbol{B} &= \begin{pmatrix} \boldsymbol{J}_B^{-1} \\ \boldsymbol{0}_{4\times3} \end{pmatrix}, \\ \boldsymbol{C} &= \begin{pmatrix} \boldsymbol{0}_{4\times3} & \boldsymbol{I}_4 \end{pmatrix}.\end{aligned} \tag{4}$$

The linearization point originates from its representation of the spacecraft's default state at the beginning of every maneuver.

B. Reaction wheels

In the control problem discussed in this paper, $\boldsymbol{u}$ represents body torque command acting on the spacecraft. The body torque is generated by applying torque on each reaction wheel $\boldsymbol{L}_{\text{RWA}} = (L_{\text{RW1}}, L_{\text{RW2}}, L_{\text{RW3}}, L_{\text{RW4}})^T$. Each reaction wheel torque contribution to body torque is given by reaction wheels assembly configuration, embedded in the control allocation matrix $\boldsymbol{W}$ [9]. Then the resulting body torque command is given by

$$\boldsymbol{u} = -\boldsymbol{W}\boldsymbol{L}_{\text{RWA}}. \tag{5}$$

The reaction wheel torque L_{RWi} is bounded. All reaction wheel array (RWA) torques are within the n-dimensional cube, defined by the reaction wheel torque constraints.

The feedback controller outputs body torque $\boldsymbol{u}$. The calculation of reaction wheels torques from body torque $\boldsymbol{u}$ is given by the control allocation matrix pseudo-inversion $\boldsymbol{W}^\dagger$ as

$$\boldsymbol{L}_{\text{RWA}} = -\boldsymbol{W}^\dagger\boldsymbol{u}. \tag{6}$$

Another constraint of the reaction wheel is the maximal momentum of the reaction wheel h_{RWi}, defined by the maximal reaction wheel speed ω_{RWi} and wheel rotor inertia.

C. Feedback control

The baseline feedback controller is derived by solving the LQR problem on a linearized model derived from the original non-linear dynamics (3). However, the linearized model defined in (4) is not controllable. State corresponding to quaternion scalar component q_0 is recomputed from vector components $q_0 = \sqrt{1 - q_1^2 - q_2^2 - q_3^2}$ that provides a controllable linearized model but introduced singularity at rotations $\pm\pi$ [8].

By approximating inertia tensor to diagonal matrix $\boldsymbol{J}_B \approx \text{diag}(\,J_{\text{xx}},\, J_{\text{yy}},\, J_{\text{zz}}\,)$, state-feedback control law for each axis separately is obtained

$$\boldsymbol{u} = -(\boldsymbol{D}\ \boldsymbol{H})(\boldsymbol{\delta\omega},\, \text{sgn}(\delta q_0)\boldsymbol{\delta q}_{1:3})^T, \tag{7}$$

where $\boldsymbol{u}$ is resulting control torque in body frame, $\boldsymbol{D}$, $\boldsymbol{H}$ are diagonal matrices, and six states $\boldsymbol{\delta\omega}$, $\boldsymbol{\delta q}$ represent error states [7] calculated as

$$\begin{aligned} \boldsymbol{\delta\omega} &= \hat{\boldsymbol{\omega}} - \boldsymbol{\omega}_{\mathrm{ref}}, \\ \boldsymbol{\delta q} &= \hat{\boldsymbol{q}} \otimes \boldsymbol{q}_{\mathrm{ref}}^{-1}. \end{aligned} \tag{8}$$

Control torque in the body frame is then transformed to reaction wheel torque using a relationship in (6). Angular rate $\hat{\boldsymbol{\omega}}$ and quaternion $\hat{\boldsymbol{q}}$ estimates are provided by navigation function which is either star tracker measurement (if available) or fusion of MEMS gyroscope, fine Sun sensor, and magnetometer measurements in the Multiplicative Extended Kalman Filter (MEKF) [7].

D. Reference shaper

A reference shaper is employed to mitigate abrupt changes in the reference which can lead to exceeding the speed limit of a maneuver. The reference shaper function provides angular rate $\boldsymbol{\omega}_{\mathrm{ref}}$ and quaternion $\boldsymbol{q}_{\mathrm{ref}}$ references for error state calculations (8). The limiter is based on the SLERP which is the spherical linear interpolation between two quaternions q_0 and q_1 over a parameter $t \in [0, 1]$. The interpolation is given by

$$\mathrm{slerp}(q_0, q_1, t) = \frac{\sin((1-t)\theta)}{\sin\theta} q_0 + \frac{\sin(t\theta)}{\sin\theta} q_1, \tag{9}$$

where $\theta = \cos^{-1}(q_0 \cdot q_1)$ is the angle between q_0 and q_1 [10].

Rate-limited quaternion $\boldsymbol{q}_{\mathrm{ref},\lim_k}$ is expressed by the following equation

$$\boldsymbol{q}_{\mathrm{ref},\lim_k} = \mathrm{slerp}(\boldsymbol{q}_{\mathrm{ref},\lim_{k-1}}, \boldsymbol{q}_{\mathrm{ref}_k}, t). \tag{10}$$

Here, $\boldsymbol{q}_{\mathrm{ref},\lim_{k-1}}$ is the rate-limited quaternion reference from the previous step, and $\boldsymbol{q}_{\mathrm{ref}_k}$ is the unconstrained reference quaternion at the current step k. Parameter t represents the interpolation factor that ensures the maneuver adheres to the maximum rotation speed limit ω_{MAX}. If $t = 0$, the resulting quaternion $\boldsymbol{q}_{\mathrm{ref},\lim_k}$ is equal to $\boldsymbol{q}_{\mathrm{ref},\lim_{k-1}}$. Conversely, when $t = 1$, the resultant $\boldsymbol{q}_{\mathrm{ref},\lim_k}$ matches $\boldsymbol{q}_{\mathrm{ref}_k}$. Parameter t is defined in each controller step as $t = \min\left(\frac{\alpha_{\mathrm{MAX}}}{\alpha_{\mathrm{act}}}, \quad 1\right)$, where α_{MAX} represents the maximum angle the spacecraft can travel in one sample time of the control loop, $\alpha_{\mathrm{MAX}} = \omega_{\mathrm{MAX}}\Delta t$. The angle α_{act} represents minimum rotation angle between the $\boldsymbol{q}_{\mathrm{ref},\lim_{k-1}}$ and $\boldsymbol{q}_{\mathrm{ref}_k}$.

III. Reference governor design

A. Inner loop

The inner loop composed from the linear dynamics (4) and state feedback gain $\boldsymbol{K}$ is given in Fig. 1. Using state feedback control, no additional states of the closed-loop system are added. The linear dynamic of the inner loop is described by the matrices $\boldsymbol{A}_{\mathrm{cl}}$, $\boldsymbol{B}_{\mathrm{cl}}$, $\boldsymbol{C}_{\mathrm{cl}}$ calculated as

$$\begin{aligned} \boldsymbol{A}_{\mathrm{cl}} &= \boldsymbol{A} - \boldsymbol{B}\boldsymbol{K}, \\ \boldsymbol{B}_{\mathrm{cl}} &= \boldsymbol{B}\boldsymbol{K}, \\ \boldsymbol{C}_{\mathrm{cl}} &= \boldsymbol{C}. \end{aligned} \tag{11}$$

The input to the system $\boldsymbol{u}$ can be computed by the relation

$$\boldsymbol{u} = \boldsymbol{K}(\boldsymbol{x}_r - \boldsymbol{x}). \tag{12}$$

The linear relationship (12) approximates non-linear error state formulation (8). In addition, LRG uses a full quaternion model with seven state variables $\boldsymbol{x}$ instead of reduced quaternions in the state-feedback control with six states. Therefore, a column with zeros is inserted for the scalar part of the quaternion q_0, which is not considered in feedback. The augmented state-feedback matrix in the LRG closed-loop model is then $\boldsymbol{K} = \begin{pmatrix} \boldsymbol{D} & \boldsymbol{0}_{3\times 1} & \boldsymbol{H} \end{pmatrix}$.

B. Optimal Control Problem formulation

We aim to design a linear reference governor for the discretized inner loop with sampling time T_s using the Zero-order Hold (ZOH) discretization method. The used control scheme can be visible in Fig. 1.

The quadratic cost function is used in the tracking formulation of the optimal control problem defined as

$$\begin{aligned} \min_{\Delta\boldsymbol{x}_r(k),\, k=1,\cdots,N} & \|\boldsymbol{e}(N)\|_{\boldsymbol{S}}^2 + \sum_{k=0}^{N-1} \|\boldsymbol{e}(k)\|_{\boldsymbol{Q}}^2 + \|\Delta\boldsymbol{x}_r(k)\|_{\boldsymbol{R}}^2 \\ \text{s.t. } & \tilde{\boldsymbol{x}}(k+1) = \tilde{\boldsymbol{A}}\tilde{\boldsymbol{x}}(k) + \tilde{\boldsymbol{B}}\Delta\boldsymbol{x}_r(k), \\ & \boldsymbol{x}(k) \in \mathcal{X}, \\ & \boldsymbol{u}(k) \in \mathcal{U}, \\ & \tilde{\boldsymbol{x}}(0) = \tilde{\boldsymbol{x}}_{t_0}. \end{aligned} \tag{13}$$

In order to reduce the number of optimization parameters, the sequential formulation is used [11].

The symbol $\tilde{\boldsymbol{x}}(k) = (\boldsymbol{x}(k), \boldsymbol{x}_r(k-1))^T$ stands for the augmented state vector, $\boldsymbol{e} = \boldsymbol{r} - \tilde{\boldsymbol{C}}\tilde{\boldsymbol{x}}$ for control error. The $\boldsymbol{S}$, $\boldsymbol{Q}$, $\boldsymbol{R}$ are diagonal matrices, N represents prediction horizon and $\tilde{\boldsymbol{x}}_0$ initial condition of the augmented system. The set $\mathcal{X}$ represents a set of all admissible states and $\mathcal{U}$ all admissible inputs in the inner loop. The linear system state-space representation matrices for the discrete-time augmented system by last input are given by

$$\begin{aligned} \tilde{\boldsymbol{A}} &= \begin{pmatrix} \boldsymbol{A}_{\mathrm{cl}} & \boldsymbol{B}_{\mathrm{cl}} \\ \boldsymbol{0} & \boldsymbol{I} \end{pmatrix}, \\ \tilde{\boldsymbol{B}} &= \begin{pmatrix} \boldsymbol{B}_{\mathrm{cl}} \\ \boldsymbol{I} \end{pmatrix}, \\ \tilde{\boldsymbol{C}} &= \begin{pmatrix} \boldsymbol{C} & \boldsymbol{0} \end{pmatrix}. \end{aligned} \tag{14}$$

C. Constraints

The constraints on the system are utilized to respect the spacecraft design limitations described earlier. These hard constraints are put on states $\boldsymbol{x}$, but also on the input of the inner system $\boldsymbol{u}$.

1) State constraints: State constraints are put just on the spacecraft rotational speed, which can be selected by $\boldsymbol{x}_\omega = \boldsymbol{E}_{\boldsymbol{\omega}}\tilde{\boldsymbol{x}}$. For the rotational speed box constraints (15) are employed

$$\boldsymbol{x}_\omega \in \{\boldsymbol{z} \in \mathbb{R}^3 \,|\, \omega_{\mathrm{MIN}} \leq \boldsymbol{z} \leq \omega_{\mathrm{MAX}}\}. \tag{15}$$

The set satisfying (15) is the solution of the set of linear inequalities

$$\boldsymbol{G}_{\omega}\boldsymbol{x}_{\omega} \leq \boldsymbol{h}_{\omega}. \tag{16}$$

Then the state constraints are added to the optimization problem as linear inequalities.

2) Input constraints: The input $\boldsymbol{u}$ of the inner loop is constrained, according to the subsection II-B. The reaction wheel angular momentum constraint will not be taken into account in the optimization, because the maximal reaction wheels angular momentum h_{RWi} is large enough, so the momentum saturation of reaction wheels, during re-orienting is not possible. As a consequence of neglecting h_{RWi} saturation, no four additional states, representing reaction wheels integrator dynamics, to the control-oriented model are added.

After incorporation of the control allocation (6), the input constraints are given in the form

$$\boldsymbol{u} \in \{\boldsymbol{z} \in \mathbb{R}^3 \,|\, \boldsymbol{L}_{\mathrm{RWA_{MIN}}} \leq \boldsymbol{W}^{\dagger}\boldsymbol{z} \leq \boldsymbol{L}_{\mathrm{RWA_{MAX}}}\}. \tag{17}$$

For each reaction wheel, two linear inequalities describe the torque constraint. For all reaction wheels throughout the prediction horizon, $8N$ linear inequalities describe torque constraints.

Constraints on $\boldsymbol{u}$ can be formulated in the form of a set of linear inequalities

$$\boldsymbol{G}_{\boldsymbol{u}}\boldsymbol{u} \leq \boldsymbol{h}_{\boldsymbol{u}} \tag{18}$$

such that its solution is set (17).

To be in line with sequential formulation, the input $\boldsymbol{u}$ throughout the prediction horizon is given by

$$\begin{aligned}
\boldsymbol{U} &= \hat{\hat{\boldsymbol{C}}} \cdot \Delta\boldsymbol{X}_r + \hat{\hat{\boldsymbol{D}}}\tilde{\boldsymbol{x}}_{t_0}, \\
\hat{\hat{\boldsymbol{C}}} &= \begin{pmatrix} \boldsymbol{K} & \boldsymbol{0} & \cdots & \boldsymbol{0} \\ \boldsymbol{\Psi}\tilde{\boldsymbol{A}}^0\tilde{\boldsymbol{B}} & \boldsymbol{K} & \ddots & \boldsymbol{0} \\ \vdots & \ddots & \ddots & \vdots \\ \boldsymbol{\Psi}\tilde{\boldsymbol{A}}^{N-2}\tilde{\boldsymbol{B}} & \cdots & \boldsymbol{\Psi}\tilde{\boldsymbol{A}}^0\tilde{\boldsymbol{B}} & \boldsymbol{K} \end{pmatrix}, \\
\hat{\hat{\boldsymbol{D}}} &= \begin{pmatrix} \boldsymbol{\Psi} \\ \boldsymbol{\Psi}\tilde{\boldsymbol{A}} \\ \vdots \\ \boldsymbol{\Psi}\tilde{\boldsymbol{A}}^{N-1} \end{pmatrix}, \\
\boldsymbol{\Psi} &= (-\boldsymbol{K}\boldsymbol{E}_{\boldsymbol{x}} + \boldsymbol{K}\boldsymbol{E}_{\boldsymbol{x}_r}),
\end{aligned} \tag{19}$$

where $\boldsymbol{U}$ represents the column vector of all inputs in the prediction horizon. Similarly, $\Delta\boldsymbol{X}_r$ stands for all state reference increments. Matrix $\boldsymbol{E}_{\boldsymbol{x}}$ selects inner loop state from the augmented state $\tilde{\boldsymbol{x}}$. Similarly matrix $\boldsymbol{E}_{\boldsymbol{x}_r}$ selects last state reference from the augmented state $\tilde{\boldsymbol{x}}$.

D. Decision variables reduction

Manipulating reference by LRG for quaternion and for the rotational speed results in the irrelevant reference signals, such that constant quaternion (zero angular rate) reference could be achieved with constant non-zero quaternion and angular rate reference combination. Optimization over full state reference violates dynamics coupling between rotational speed and quaternion. To add this coupling into the optimization problem the number of optimization variables was reduced by optimizing over reduced quaternion reference increment $\Delta\boldsymbol{x}_{r_q}$. From this, the full state reference signal increment is computed using relation $\Delta\boldsymbol{x}_r = \boldsymbol{E}\Delta\boldsymbol{x}_{r_q}$, where $\boldsymbol{E} = \begin{pmatrix} \boldsymbol{0}_{4\times3} \\ \boldsymbol{I}_3 \end{pmatrix}$. Based on the discretized linear model, the rotational speed reference can be computed using $\Delta\boldsymbol{x}_{r_q}$ as

$$\boldsymbol{x}_{r_\omega} = \boldsymbol{A}_{q,\omega}^{-1}\Delta\boldsymbol{x}_{r_q}. \tag{20}$$

Rotational speed computation (20) influences the augmented system dynamics. Let us split the matrices $\boldsymbol{A}_{\mathrm{cl}}$, $\boldsymbol{B}_{\mathrm{cl}}$ by selecting specific rows and columns, into $\boldsymbol{A}_{q,\omega}$, $\boldsymbol{B}_{\omega,\boldsymbol{x}_{r_\omega}}$, $\boldsymbol{B}_{\omega,\boldsymbol{x}_{r_q}}$ as

$$\begin{aligned}
\boldsymbol{A}_{q,\omega} &= \boldsymbol{A}_{\mathrm{cl}_{(5:7,1:3)}}, \\
\boldsymbol{B}_{\omega,\boldsymbol{x}_{r_\omega}} &= \boldsymbol{B}_{\mathrm{cl}_{(1:3,1:3)}}, \\
\boldsymbol{B}_{\omega,\boldsymbol{x}_{r_q}} &= \boldsymbol{B}_{\mathrm{cl}_{(1:3,5:7)}}, \\
\boldsymbol{B}_{\boldsymbol{x}} &= \begin{pmatrix} \boldsymbol{B}_{\omega,\boldsymbol{x}_{r_q}} & \boldsymbol{0}_{4\times3} \end{pmatrix}^T, \\
\boldsymbol{B}_{\boldsymbol{x}_r} &= \begin{pmatrix} \boldsymbol{B}_{\omega,\boldsymbol{x}_{r_\omega}}\boldsymbol{A}_{q,\omega}^{-1} + \boldsymbol{B}_{\omega,\boldsymbol{x}_{r_q}} & \boldsymbol{0}_{4\times3} \end{pmatrix}^T.
\end{aligned} \tag{21}$$

Then the changed matrices of augmented system $\tilde{\boldsymbol{A}}$, $\tilde{\boldsymbol{B}}$ are designed in the following manner

$$\begin{aligned}
\tilde{\boldsymbol{A}} &= \begin{pmatrix} \boldsymbol{A}_{\mathrm{cl}} & \boldsymbol{B}_{\boldsymbol{x}} \\ \boldsymbol{0} & \boldsymbol{I} \end{pmatrix}, \\
\tilde{\boldsymbol{B}} &= \begin{pmatrix} \boldsymbol{B}_{\boldsymbol{x}_r} \\ \boldsymbol{I} \end{pmatrix}.
\end{aligned} \tag{22}$$

The matrix $\hat{\hat{\boldsymbol{C}}}$ is also influenced by the dynamics change

$$\begin{aligned}
\hat{\hat{\boldsymbol{C}}} &= \begin{pmatrix} \boldsymbol{K}\boldsymbol{F} & \boldsymbol{0} & \cdots & \boldsymbol{0} \\ \boldsymbol{\Psi}\tilde{\boldsymbol{A}}^0\tilde{\boldsymbol{B}} & \boldsymbol{K}\boldsymbol{F} & \ddots & \boldsymbol{0} \\ \vdots & \ddots & \ddots & \vdots \\ \boldsymbol{\Psi}\tilde{\boldsymbol{A}}^{N-2}\tilde{\boldsymbol{B}} & \cdots & \boldsymbol{\Psi}\tilde{\boldsymbol{A}}^0\tilde{\boldsymbol{B}} & \boldsymbol{K}\boldsymbol{F} \end{pmatrix}, \\
\boldsymbol{\Psi} &= (-\boldsymbol{K}\boldsymbol{E}_{\boldsymbol{x}} + \boldsymbol{K}\boldsymbol{E}\boldsymbol{E}_{\boldsymbol{x}_{r_q}}), \\
\boldsymbol{F} &= \begin{pmatrix} \boldsymbol{A}_{q,\omega}^{-1} \\ \boldsymbol{0}_{1\times3} \\ \boldsymbol{I}_3 \end{pmatrix}.
\end{aligned} \tag{23}$$

Matrix $\boldsymbol{E}_{\boldsymbol{x}_{r_q}}$ selects the reduced quaternion reference from augmented state vector $\tilde{\boldsymbol{x}}$.

IV. Numerical simulation

A. Simulation setup

The LRG was verified in a high-fidelity simulator, which uses accurate non-linear models representing spacecraft and environmental dynamics. The simulation was conducted using NASA's software *42* [12]. The LRG was integrated into Flight Software (FSW) implemented in MATLAB, interfaced with *42* through inter-process communication (IPC). All environmental disturbances were enabled and all used equipment (sensors,

actuators) parameters were set up according to real performances, including noise. For details on environmental torques and noise levels, see [13] and [12]. We used the model of FSW and the simulation environment setup designed for nominal operations for the upcoming VZLU AEROSPACE Cubesat mission. The FSW implements sensor measurement processing, navigation, guidance, control, and actuator commanding functions.

Proposed LRG replaces the default reference shaper function, generating quaternion trajectory based on the SLERP algorithm and feeding the reference angular rate and quaternion references to the state-feedback controller (7). Otherwise, the FSW and simulation scenario were set up identically in the verification simulations.

Each reaction wheel torque is limited in the range $-0.002 \leq L_{\text{RWi}} \leq 0.002$ Nm, and angular rate about all axes shall be bounded in the range $-3 \leq \boldsymbol{x}_\omega \leq 3$ °/s. The angular rate limit for SLERP is also set to $\omega_{\text{MAX}} = 3$ °/s. The FSW runs at $T_s = 0.2$ seconds sampling rate (including LRG). LRG is parametrized with prediction horizon $N = 20$ samples and weighting matrices $\boldsymbol{Q} = \text{diag}(0.1,\ 1,\ 1,\ 1)$, $\boldsymbol{S} = \text{diag}(10,\ 10,\ 10,\ 10)$, $\boldsymbol{R} = \text{diag}(10,\ 10,\ 10)$.

Slew maneuver duration is determined by the entry and exit conditions. The slew is started when the tracking error angle is ≥ 6 °. The slew is exited when the tracking error angle is ≤ 5.5 °, and the spacecraft angular rate magnitude is ≤ 1 °/s.

B. Verification

The simulation scenario initial condition was specified at the linearization point zero angular rate $\boldsymbol{\omega}_0 = (0, 0, 0)^T$ °/s and unit quaternion $\boldsymbol{q}_0 = (1, 0, 0, 0)^T$. All reaction wheels start at zero speed; the FSW's momentum management drives them toward nominal speeds, resulting in initial non-zero torque at the beginning of the simulation.

1) Rotation about single axis: The spacecraft was requested to rotate by 120 ° about X-axis at time $t_{\text{man}} = 20$ seconds which gives desired quaternion $\boldsymbol{q}_r = (0.5\ 0.866\ 0\ 0)^T$ at $t \geq t_{\text{man}}$. The time-domain profile of the maneuver is shown in Fig. 2. The slew maneuver was finished in 41.4 seconds. Thanks to the reference preview information, the maneuver was started before the actual reference was requested. Angular rate state constraint was reached but later violated as the spacecraft states were drifting away from the linearization point.

2) Rotation about all axes: The spacecraft is requested to rotate by total angle 120° distributed to all axes at time $t_{\text{man}} = 20$ seconds which gives desired quaternion $\boldsymbol{q}_r = (0.5\ 0.5\ 0.5\ 0.5)^T$ at $t \geq t_{\text{man}}$. The time-domain profile of the maneuver is shown in Fig. 3. The slew maneuver was finished in 28.2 seconds. Similarly to the single axis rotation scenario, the angular rate state constraint was firstly reached but later violated as the spacecraft states were drifting away from the linearization point. In this case, RW torque limits were active and not violated.

3) Reference shaper - Rotation about single axis: This scenario shows the default reference shaper functionality in

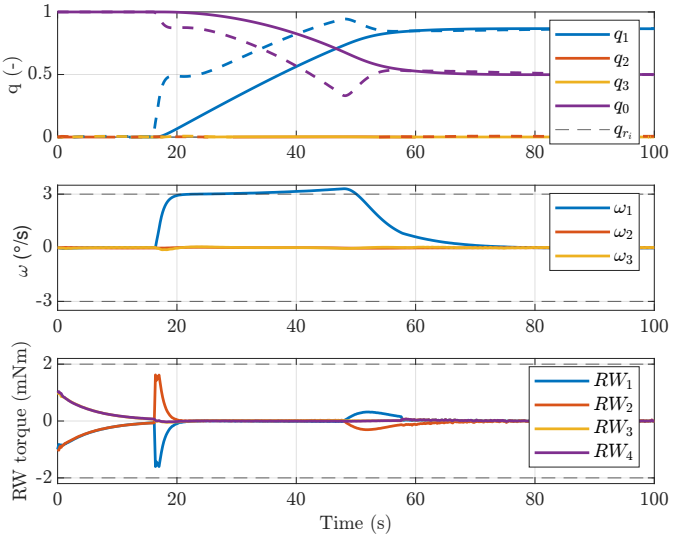

Fig. 2. Reference governor repoints the spacecraft by 120 ° about X axis by manipulating the quaternion state reference $\boldsymbol{x}_{r_q}$ (dashed line). The slew maneuver was started at time 16.4 second and finished at 57.8 second. An angular rate state constraint of 3 °/s was reached but it was also violated by a maximum of 0.3 °/s due to linearization error. Reaction wheel torque limits were not reached.

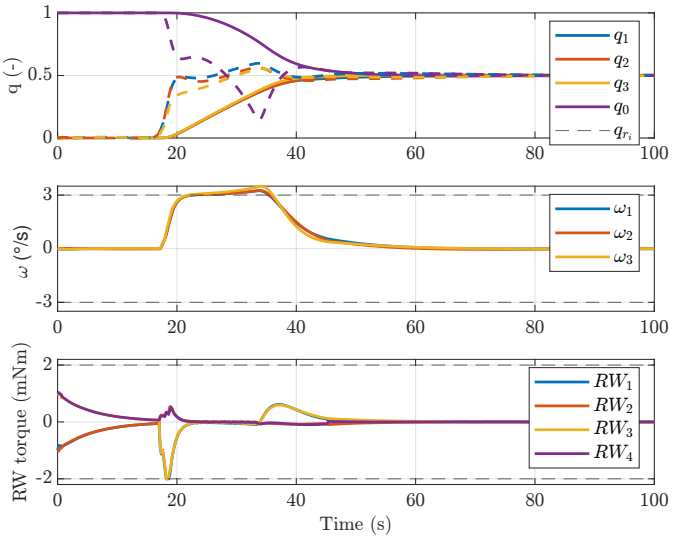

Fig. 3. Reference governor repoints the spacecraft by total angle 120 ° distributed to all axes by manipulating the quaternion state reference $\boldsymbol{x}_{r_q}$ (dashed line). The slew maneuver was started at time 17.2 second and finished at 45.4 second. An angular rate state constraint of 3 °/s was reached but it was also violated by a maximum of 0.5 °/s due to linearization error. Reaction wheel torque limits were reached and satisfied.

the rotation by 120 ° about the X-axis at time $t_{\text{man}} = 20$ seconds. The time-domain profile of the maneuver is shown in Fig. 4. The slew maneuver was finished in 59.6 seconds. Since quaternion generated trajectory neglects spacecraft dynamics, an infeasible 3 °/s angular rate is immediately requested. The controller then violates the 3 °/s rate limit by 0.45 °/s to catch up with running quaternion. At the same time, the acceleration/deceleration does not utilize full reaction wheel torque

capacity which prevents reaching faster attitude maneuvers. From this transient an overshoot using the SLERP algorithm is visible, resulting in a longer settling time, which can be seen in the Fig. 5.

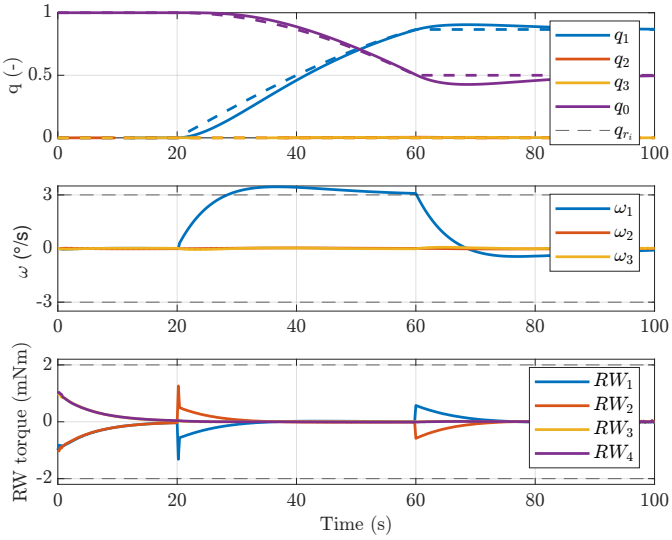

Fig. 4. Reference shaper repoints the spacecraft by 120 ° about X-axis by generating quaternion reference trajectory $\boldsymbol{x}_{r_q}$ (dashed line) at specified rate 3 °/s. The slew maneuver was started at time 20.4 second and finished at 80 second. An angular rate up to 3.45 °/s was reached to catch up with the generated trajectory since the trajectory did not respect spacecraft dynamics acceleration/deceleration. Reaction wheel torque limits were not reached.

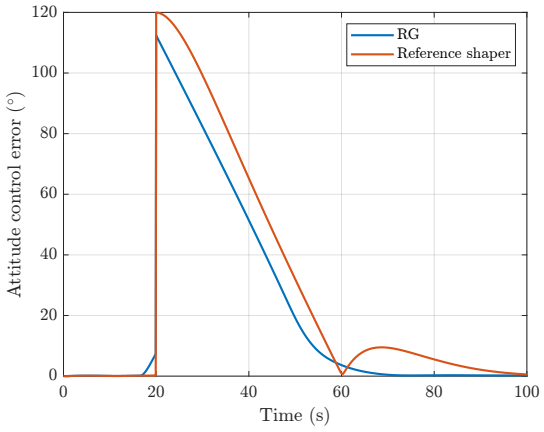

Fig. 5. Comparison of LRG and reference shaper. The attitude reference was changed by 120 ° about the X-axis. The effect of reference preview implemented in LRG is visible, spacecraft starts maneuvering in advance. Also, the long settling time of FSW with reference shaper can be seen.

V. Conclusion

This paper has presented the solution to the rate-limited attitude maneuvers in the form of the Linear Reference Governor approach. The proposed LRG algorithm modifies reduced quaternion and angular rate references to the attitude state-feedback controller while incorporating spacecraft angular rate and reaction wheel torque constraints. The solution relies on a linear approximation of the problem, allowing it to formulate as a Quadratic Program, which is efficiently solved online.

Using this QP formulation and the algorithm already implemented in the FSW allows VZLU AEROSPACE to straightforwardly deploy the designed algorithm on one of the upcoming Cubesat missions.

The performance of the LRG is validated in high-fidelity simulations in two scenarios with 120 ° angle rotations from the initial conditions. Significantly faster slews (53% faster than SLERP in case of single axis rotation) were achieved compared to default quaternion-based trajectory generation based on SLERP. However, an apparent drawback of the linearization was observed that the angular rate constraints in non-linear simulation were violated. This behavior does not significantly affect the mission. Reaction wheel torque constraints were not violated.

Further development of the LRG method should include linearized model updates at each step to avoid model mismatch and consequent violations of the angular rate constraints. Exclusion zone constraints could be also added to the problem to avoid potential blinding of the star tracker due to the Sun or Earth's stray light.

References

[1] Henri C Kjellberg and E Glenn Lightsey. Discretized constrained attitude pathfinding and control for satellites. *Journal of Guidance, Control, and Dynamics*, 36(5):1301–1309, 2013.

[2] Rui Xu, Yuqi Fan, Zhaoyu Li, Shengying Zhu, Haibin Shang, and Ai Gao. Time-optimal attitude planning for spacecraft with movable parts using second order cone programming. *Aerospace Science and Technology*, 141:108589, 2023.

[3] Laurent Burlion, Jean-Marc Biannic, and Tarek Ahmed-Ali. Attitude tracking control of a flexible spacecraft under angular velocity constraints. *International Journal of Control*, 92(7):1524–1540, 2019.

[4] Abhijit Dongare, Reza Hamrah, and Amit K Sanyal. Attitude pointing control using artificial potentials with control input constraints. In *2021 American Control Conference (ACC)*, pages 1–6. IEEE, 2021.

[5] Marco M Nicotra, Dominic Liao-McPherson, Laurent Burlion, and Ilya V Kolmanovsky. Spacecraft attitude control with nonconvex constraints: An explicit reference governor approach. *IEEE Transactions on Automatic Control*, 65(8):3677–3684, 2019.

[6] Uroš Kalabić, Rohit Gupta, Stefano Di Cairano, Anthony Bloch, and Ilya Kolmanovsky. Constrained spacecraft attitude control on so (3) using reference governors and nonlinear model predictive control. In *2014 American Control Conference*, pages 5586–5593. IEEE, 2014.

[7] F. L. Markley and J. Crassidis. *Fundamentals of Spacecraft Attitude Determination and Control*. Springer New York, 2014.

[8] Y. Yang. *Spacecraft Modeling, Attitude Determination, and Control Quaternion-based Approach*. CRC Press, 2019.

[9] F Landis Markley, Reid G Reynolds, Frank X Liu, and Kenneth L Lebsock. Maximum torque and momentum envelopes for reaction wheel arrays. *Journal of Guidance, Control, and Dynamics*, 33(5):1606–1614, 2010.

[10] Ken Shoemake. Animating rotation with quaternion curves. *ACM Transactions on Graphics*, 19(3), 1985.

[11] James Blake Rawlings, David Q Mayne, Moritz Diehl, et al. *Model Predictive Control: Theory, Computation, and Design*, volume 2. Nob Hill Publishing Madison, WI, 2017.

[12] E. Stoneking. 42: An open-source simulation tool for study and design of spacecraft attitude control systems. Technical report, NASA, 2018.

[13] Dávid Hriadel, Dominik Beňo, Rudolf Andoga, and Martin Hromčík. Perspective methods for high performance cubesat attitude control. In *2024 New Trends in Aviation Development (NTAD)*, pages 62–67, 2024.